Proceedings Paper:

Harput, S orcid.org/0000-0003-0491-4064, McLaughlan, J, Freear, S orcid.org/0000-0001-7858-4155 et al. (6 more authors) (2015) Nonlinear Generation of Harmonic Content within High Intensity Ultrasound Signals using Granular Chains. In: 2015 IEEE International Ultrasonics Symposium (IUS). , 21-24 Oct 2015, Taipei, Taiwan. IEEE . ISBN 978-1-4799-8182-3

https://doi.org/10.1109/ULTSYM.2015.0191

Nonlinear Generation of Harmonic Content within High Intensity Ultrasound Signals using Granular Chains

Sevan Harput, James McLaughlan, and Steven Freear
Ultrasonics and Instrumentation Group, School of Electronic and Electrical Engineering, University of Leeds, Leeds, LS2 9JT, UK
E-mail: S.Harput@leeds.ac.uk

Pierre Gelat, and Nader Saffari
Department of Mechanical Engineering, University College London, Torrington Place, London WC1E 7JE, UK

Jia Yang, Omololu Akanji, Peter J. Thomas, and David A. Hutchins
School of Engineering, University of Warwick, Coventry CV4 7AL, UK

***Abstract*—Applications such as High Intensity Focused Ultrasound (HIFU) conventionally use narrowband signals of high amplitude, which are then focused to a known region within the body. It would be advantageous to be able to broaden the bandwidth, as this could lead to a more spatially-concentrated focal region. One way of increasing the bandwidth is to generate harmonics. The eventual aim of this study is to generate wideband ultrasonic signals with high amplitudes, primarily for therapeutic ultrasound and drug delivery applications. In this paper, a new ultrasonic transducer technology using a one-dimensional chain of spheres is presented to achieve this aim.**

I. Introduction

Generation of short duration ultrasonic pulses is desirable both in diagnostic and therapeutic ultrasound. In diagnostic imaging, wideband pulses improve image resolution and can increase the potential of harmonic imaging and multiple excitation techniques [1]–[3]. In ultrasound therapy, short duration high-pressure ultrasound pulses create a compact, dense high energy region and reduce the possibility of hot-spots by reducing undesirable constructive interference. In histotripsy, short duration negative monopolar pulses can inhibit shock scattering [4], [5]. In High Intensity Focused Ultrasound (HIFU), a precise control on the focal region is necessary to minimise the potential collateral damage in the surrounding healthy tissue.

A new ultrasonic transducer technology to generate wideband impulses using a one-dimensional chain of spheres is presented recently. An ultrasonic horn is used to generate high amplitude narrow band sinusoidal signals [6]. The Hertzian contact between the spheres causes the nonlinearity of the system to increase. As a result of high nonlinearity and dispersion in this granular chain of spheres, elastic *solitary* wave generation is achieved. The propagation characteristics of the solitary waves can be tuned by changing the pre-compression force in the chain, which makes it suitable for focusing and steering of ultrasound waves [7], [8].

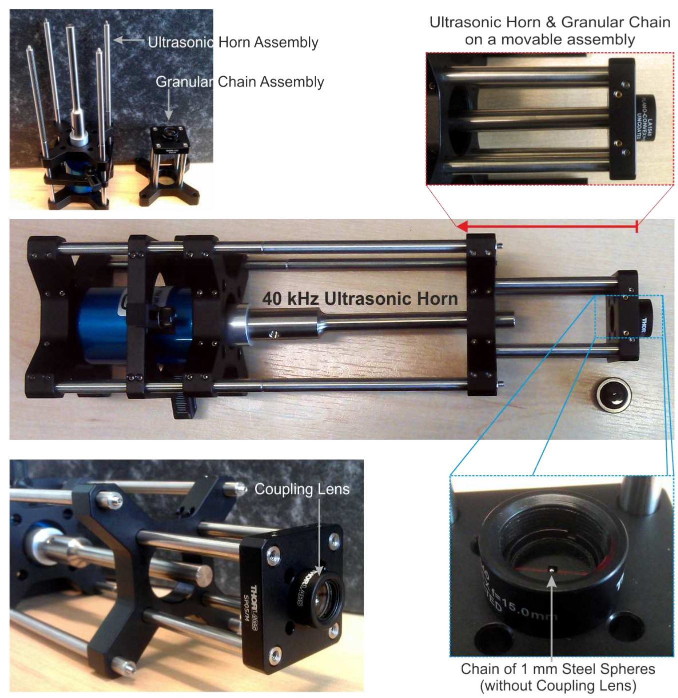

Fig. 1. Granular chain and the ultrasonic horn assembly.

The aim of this study was to generate a set of transient wide bandwidth impulses with high amplitudes similar to solitary waves, primarily for therapeutic ultrasound and drug delivery applications. It has already been demonstrated by Hutchins *et al.* and Yang *et al.* that it was possible to generate wideband impulses by coupling energy from the fundamental frequency to the harmonics at an excitation frequency of 73 kHz [6], [9], [10]. This study is based on a similar granular chain setup, but utilizing higher frequencies to achieve similar nonlinear effects in a chain of spheres and hence generation of higher order harmonics at low MHz range.

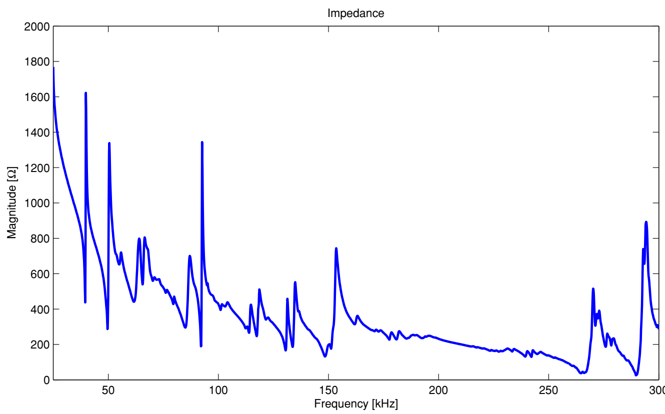

Fig. 2. Impedance plot of the 40 kHz ultrasonic horn.

II. Materials and Methods

A titanium-alloy ultrasonic process horn with a fundamental frequency of 40 kHz was used to generate narrowband signals for input into the chain of spheres. Figure 1 shows the granular chain and the ultrasonic horn assembly. The holder for the spheres was printed by using the Digital Light Processing (DLP) technique using an EnvisionTEC Perfactory Mini Multi Lens 3D Printer (Envisiontec Inc., Dearborn, MI) with properties similar to acrylic (Young's modulus 3 GPa and Poisson's ratio 0.35). The chain consisted of 6, 7, or 8 spheres of 316 stainless steel with a diameter of 1 mm, density of 7833 kg/m^3, Young's modulus 201 GPa, and Poisson's ratio 0.3, was placed into this holder. The end of the chain was terminated with a matching layer, a 0.5 mm thick Sigradur K disc with a Young's modulus 35 GPa and a Poisson's ratio 0.15, to increase the coupling into the water.

Both assemblies holding the chain of spheres and the ultrasonic horn was slid in (Figure 1 top-right) and held vertically under gravity loading to apply a small static force between each sphere, approximately 1.2 Newtons. After applying a desired pre-compression force, both setup were screwed and fixed together. Finally, the system was partially submersed and the output was measured in water using a Polyvinylidene Fluoride (PVDF) differential membrane hydrophone (Precision Acoustics Ltd., Dorchester, UK).

In order to select suitable working frequencies, the impedance of the 40 kHz ultrasonic horn was measured as given in Figure 2. The frequencies of 40, 50, 90, 150, and 265 kHz were chosen as the driving frequency, where the ultrasonic horn has its series resonance peaks. A sinusoidal tone burst with varying durations between 5 and 50 cycles

TABLE I
Peak-to-Peak Velocity Output of the Ultrasonic Horn for Various Excitation Frequencies

	40 kHz	50 kHz	90 kHz	150 kHz	265 kHz
20 cycles	0.53 m/s	0.23 mm/s	0.48 m/s	0.20 m/s	0.53 m/s
50 cycles	0.85 m/s	0.47 mm/s	0.60 m/s	0.30 m/s	0.70 m/s

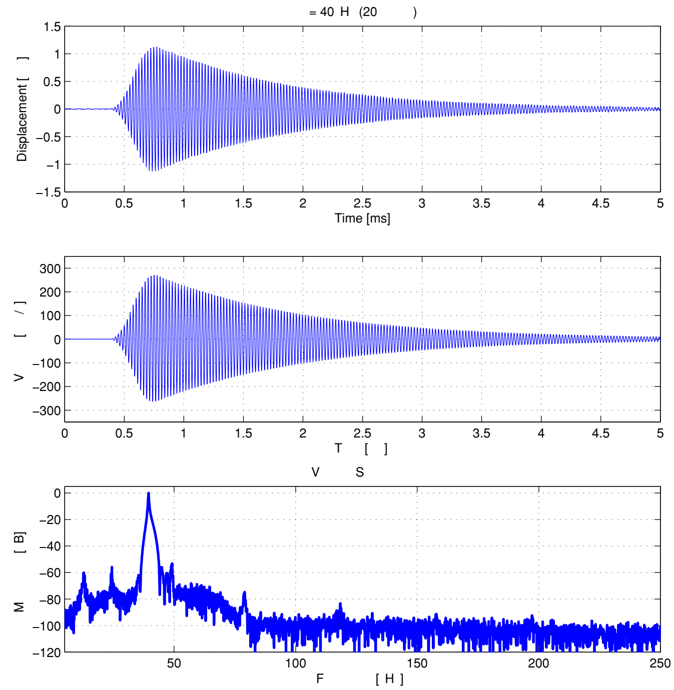

Fig. 3. (Top) Displacement and (Middle) velocity output of ultrasonic horn at 40 kHz for 20 cycles and 600 Vpp excitation. (Bottom) The spectra of the velocity output.

was used for excitation at chosen frequencies. Although the output displacement of the horn drops by increasing frequency, the generation of high frequency components increases by increasing the input frequency; *e.g.* in order to couple energy to the MHz range, the generation of the first 4 harmonics at 265 kHz is sufficient.

The input signals to the ultrasonic horn were generated by a 33600A TrueForm Waveform Generator (Agilent Technologies Inc., Santa Clara, CA) and then amplified by a 2200L Power Amplifier (Electronics & Innovation Ltd., Rochester, NY). Table I shows the peak to peak velocity profile measured at the tip of the ultrasonic horn by a PSV-500 Scanning Vibrometer (Polytec GmbH Waldbronn, Germany) at different frequencies for 600 Vpp excitation, which was the maximum input voltage used during experiments.

Figure 3 shows the input displacement and velocity profile to the granular chain measured at the tip of the ultrasonic horn and its spectrum. This vibrometer measurement performed for a 40 kHz input is a good demonstration of the output characteristic of the ultrasonic horn. The amplification effect of the horn can be observed through the first 15 cycles approximately, which is followed by a long ringing even after the 20 cycle excitation signal. Although the output displacement and velocity profiles look different than 20 cycle tone burst excitation, the spectra of the output signal shows a narrowband behaviour with subharmonic and higher harmonic levels lower than -55 dB and -74 dB, respectively.

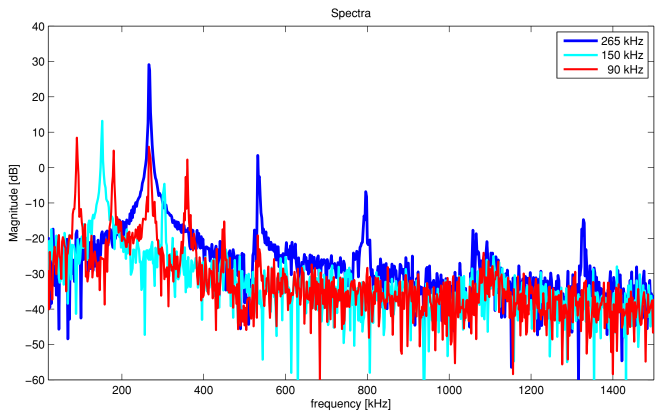

Fig. 4. Spectra of hydrophone measurements for an input excitation of 600 Vpp and 50 cycles at 90 kHz, 150 kHz, and 265 kHz.

III. Results and Discussion

There was no significant difference between the measurements performed with 6 and 7 sphere granular chains. The pressure measured for the 8 sphere granular chain setup was significantly lower than the shorter chains. It is hard to draw conclusions from limited number of measurements, but we believe that the length of the chain does not completely change the characteristics of wave propagation but increases the nonlinearities and the attenuation, where solitary wave propagation in 1D chains significantly changes with the chain length [11]. Therefore, only measurements performed with a 7 sphere granular chain is presented in this section.

The excitation lengths of 5, 10, 20 and 50 cycles were used during the measurements. However only results relating to 50 cycles excitation were presented due to the following reason; the amplification effect of the ultrasonic horn to maximise the velocity output of the horn as presented in Figure 3.

For all excitation frequencies, the Hertzian contact between adjacent spheres caused the nonlinearity of the system to increase as the signal travelled along the chain. After propagating in the chain, the narrowband sinusoidal excitation waveform was thus transformed into a signal with a greatly-extended bandwidth. Figure 4 shows the spectra of hydrophone measurements at 90 kHz, 150 kHz, and 265 kHz for 50 cycles and 600 Vpp excitation, where the relating velocity input values to the chain are listed in Table I. The results acquired using 40 kHz and 50 kHz excitations are not presented for two reasons. First, the higher order harmonics generated by these two excitations barely reached over 265 kHz, which is a big limitation for most biomedical applications. Secondly, the hydrophone was calibrated down to 300 kHz and there is a drop in hydrophone sensitivity below this value.

Figure 5 (top) shows the received signal only after 190 μs, because the electromagnetic interference caused by the power amplifier reduces the SNR significantly during the excitation. The signal envelope is different than the horn output given in Figure 3 and also it changed between consecutive measurements, but the waveform shape and harmonic levels stayed

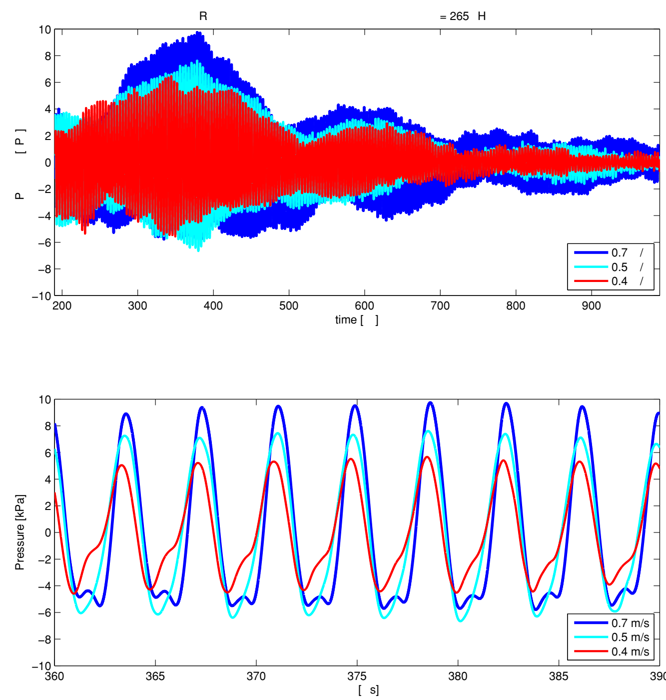

Fig. 5. Hydrophone measurements at 265 kHz for various excitation velocities.

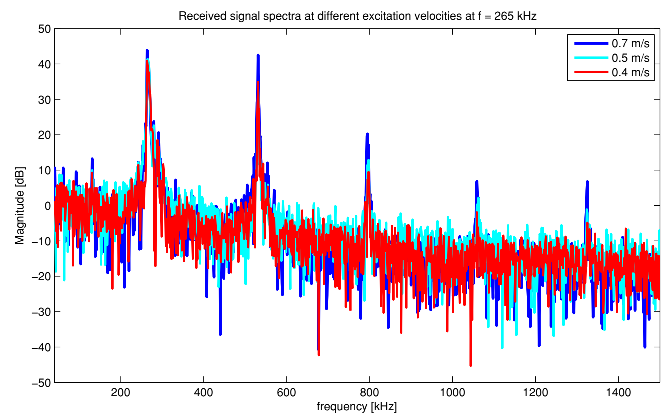

Fig. 6. Spectra of hydrophone measurements at 265 kHz for various excitation velocities.

similar during measurements. Figure 5 (bottom) zooms into a few cycles around 375 μs to show the generation of a *shocked* waveform at a pressure level as low as 10 kPa, which clearly shows that the harmonic generation is not due to the nonlinear propagation in water.

Figure 6 shows the spectra of hydrophone measurements given in Figure 5 (top). Although the peak pressure levels are linearly proportional with increasing velocity values (Figure 5), the level of higher harmonics increase approximately 10 dB between input velocities of 0.4 m/s and 0.7 m/s (Figure 6) due to the nonlinearity in the chain.

For the highest frequency and highest input velocity to the chain (f = 265 kHz, v = 0.7 m/s), the received signal accommodates higher order harmonics that extended to frequencies above 1 MHz and shows the potential of this new technology for biomedical ultrasound applications.

IV. Conclusions

The generation of higher and lower order harmonics are possible by using granular chains. However, this work focused on generation of higher order harmonics that will reach to low MHz range instead of generation of solitary waves. It is possible to generate high pressure and high frequency ultrasound waves in water at biomedical ultrasound range by using the current technology, but is necessary to improve the input velocity and frequency of the excitation transducer.

The main limitation while choosing an appropriate excitation transducer or an actuator is the trade-off between frequency and output displacement. The energy coupling to the MHz range is easier by using a high frequency input ($>$250 kHz); however high frequency transducers produce low output displacement and velocity profiles. For this reason, a 40 kHz ultrasonic horn was used at 265 kHz in this study. This is not an ideal solution to generate high displacement, because driving the ultrasonic horn out of its operating regime might also be contributing to harmonic generation. It was not possible to characterise the harmonic content of the velocity output for 265 kHz input excitation, because the vibrometer was limited to 1 MHz maximum sampling frequency.

Repeatability of the measurements for different chain lengths is another issue. The printing precision of DLP 3D printer was 15 μm, which will result in 1.5% error for a channel diameter of 1 mm and can significantly increase the static friction between the holder and stainless steel spheres. It may be the reason for the 8 spheres granular chain resulting in a significantly lower pressure than other chain lengths. High static friction also increases the effective pre-compression and input force necessary to start the propagation. To increase the efficiency of the energy coupling into higher frequencies, the pre-compression force should be reduced to increase the nonlinearities in the chain [6]. However, the cut off frequency of the granular chain gets lower by reducing the pre-compression force. Therefore, in order to achieve a wider bandwidth signals smaller diameter spheres must be used.

For therapeutic application, the main drawback of the current experimental setup is the low acoustic pressure. Most of the therapeutic ultrasound applications require a peak negative pressure greater than 1 MPa at MHz range. Therefore, next step will be building an array of granular chains to increase the output pressure of the system. For imaging applications, the main drawback is the incapability of single pulse generation. This issue can be solved by using coded excitation techniques, where coding algorithms can work for highly nonlinear processes such as imaging with ultrasound contrast agents [12].

Acknowledgment

The authors gratefully acknowledge funding from the Engineering and Physical Sciences Research Council (UK) via grant number EP/K029835/1.

References

[1] P. N. Burns, S. R. Wilson, and D. H. Simpson, “Pulse inversion imaging of liver blood flow: Improved method for characterizing focal masses with microbubble contrast,” *Investigative Radiology*, vol. 35, no. 1, pp. 58–71, 2000.

[2] Q. Ma, Y. Ma, X. Gong, and D. Zhang, “Improvement of tissue harmonic imaging using the pulse-inversion technique,” *Ultrasound in Medicine & Biology*, vol. 31, no. 7, pp. 889–894, 2005.

[3] S. Harput, J. McLaughlan, D. M. J. Cowell, and S. Freear, “Superharmonic imaging with chirp coded excitation: Filtering spectrally overlapped harmonics,” *Ultrasonics, Ferroelectrics and Frequency Control, IEEE Transactions on*, vol. 61, no. 11, pp. 1802–1814, 2014.

[4] K.-W. Lin, T. Hall, R. McGough, Z. Xu, and C. Cain, “Synthesis of monopolar ultrasound pulses for therapy: The frequency-compounding transducer,” *Ultrasonics, Ferroelectrics, and Frequency Control, IEEE Transactions on*, vol. 61, no. 7, pp. 1123–1136, 2014.

[5] K.-W. Lin, Y. Kim, A. Maxwell, T.-Y. Wang, T. Hall, Z. Xu, J. Fowlkes, and C. Cain, “Histotripsy beyond the intrinsic cavitation threshold using very short ultrasound pulses: microtripsy,” *Ultrasonics, Ferroelectrics, and Frequency Control, IEEE Transactions on*, vol. 61, no. 2, pp. 251–265, 2014.

[6] D. A. Hutchins, J. Yang, O. Akanji, P. J. Thomas, L. A. J. Davis, S. Freear, S. Harput, N. Saffari, and P. Gelat, “Evolution of ultrasonic impulses in chains of spheres using resonant excitation,” *EPL (Europhysics Letters)*, vol. 109, no. 5, p. 54002, 2015.

[7] A. Spadoni and C. Daraio, “Generation and control of sound bullets with a nonlinear acoustic lens,” *Proceedings of the National Academy of Sciences*, vol. 107, no. 16, pp. 7230–7234, 2010.

[8] C. M. Donahue, P. W. J. Anzel, L. Bonanomi, T. A. Keller, and C. Daraio, “Experimental realization of a nonlinear acoustic lens with a tunable focus,” *Applied Physics Letters*, vol. 104, no. 1, p. 014103, 2014.

[9] J. Yang, O. Akanji, D. Hutchins, P. Thomas, L. Davis, S. Freear, S. Harput, N. Saffari, and P. Gelat, “Time-delay estimation and correlation analysis of acoustic signals in granular media using wavelet decomposition,” in *Ultrasonics Symposium (IUS), 2014 IEEE International*, 2014, pp. 2529–2532.

[10] D. Hutchins, J. Yang, O. Akanji, L. Davis, P. Thomas, S. Freear, S. Harput, N. Saffari, and P. Gelat, “The study of chain-like materials for use in biomedical ultrasound,” in *Ultrasonics Symposium (IUS), 2014 IEEE International*, 2014, pp. 2607–2610.

[11] D. A. Hutchins, J. Yang, O. Akanji, P. J. Thomas, L. A. J. Davis, S. Freear, S. Harput, N. Saffari, and P. Gelat, “The generation of impulses from narrow bandwidth signals using resonant spherical chains,” in *Ultrasonics Symposium (IUS), 2015 IEEE International*, 2015.

[12] S. Harput, M. Arif, J. McLaughlan, D. M. J. Cowell, and S. Freear, “The effect of amplitude modulation on subharmonic imaging with chirp excitation,” *Ultrasonics, Ferroelectrics and Frequency Control, IEEE Transactions on*, vol. 60, no. 12, pp. 2532–2544, 2013.